Appl. Sci. **2015**, *5*, 1869-1881; doi:10.3390/app5041869

OPEN ACCESS

applied sciences

ISSN 2076-3417

www.mdpi.com/journal/applsci

Article

Kinetic Adsorption Study of Silver Nanoparticles on Natural Zeolite: Experimental and Theoretical Models

Alvaro Ruíz-Baltazar [†,*] **and Ramiro Pérez** [†]

Centro de Física Aplicada y Tecnología Avanzada, Universidad Nacional Autónoma de Mexico, Querétaro, Qro. 76230, Mexico; E-Mail: ramiro@fata.unam.mx

† These authors contributed equally to this work.

* Author to whom correspondence should be addressed; E-Mail: alvarodejesusruiz@yahoo.com.mx; Tel.: +52-44-3225-6994.

Academic Editor: Philippe Lambin

Received: 6 September 2015 / Accepted: 1 December 2015 / Published: 16 December 2015

Abstract: In this research, the adsorption capacity of Ag nanoparticles on natural zeolite from Oaxaca is presented. In order to describe the adsorption mechanism of silver nanoparticles on zeolite, experimental adsorption models for Ag ions and Ag nanoparticles were carried out. These experimental data obtained by the atomic absorption spectrophotometry technique were compared with theoretical models such as Lagergren first-order, pseudo-second-order, Elovich, and intraparticle diffusion. Correlation factors R^2 of the order of 0.99 were observed. Analysis by transmission electron microscopy describes the distribution of the silver nanoparticles on the zeolite outer surface. Additionally, a chemical characterization of the material was carried out through a dilution process with lithium metaborate. An average value of 9.3 in the Si/Al ratio was observed. Factors such as the adsorption behavior of the silver ions and the Si/Al ratio of the zeolite are very important to support the theoretical models and establish the adsorption mechanism of Ag nanoparticles on natural zeolite.

Keywords: kinetic adsorption; clinoptilolite; Ag nanoparticles; theoretical models

---

1. Introduction

Natural zeolites have been extensively studied due to their structural characteristics and physico-chemical properties. These minerals present a great porosity and a significant cation-exchange capacity [1,2]. Because of this, natural zeolites offer a wide range of applications, and one of the most notable is the removal of contaminant ions in water and soil [3–5]. It is reported that natural zeolites, specifically clinoptilolite, have been used in the removal of Mn, Cu, Ar, Pd, Cd, and Zn [4–6]. However, it is important to study the rate of adsorption of these species, in order to provide the optimum conditions for the adsorption process. The nature of the sorption process will depend on physical or chemical characteristics of the adsorbent systems and the system conditions. The most commonly used kinetic expressions to explain the solid/liquid adsorption processes are the pseudo-first-order kinetic and pseudo-second-order kinetic models [7–10]. A good number of works were reported where the modifications of these natural clays with nanoparticles were produced to carry out the adsorption of metals from aqueous solutions [8,11–18]. These minerals offer low-cost, effective supports for nano-scale entities. The reactivity of nano-scale zero-valent metals such as Ag and the high cation-exchange capacity of the zeolites represent a potential alternative for remediation applications [7,13,14,19]. However, specific studies about kinetics adsorption of nanoparticles on clinoptilolite have not been explored thoroughly. In this research the chemical characterization and the synthesis methodology of the composite of silver nanoparticle AgNPs-zeolite is presented. Additionally, a detailed analysis of the kinetics of adsorption of Ag nanoparticles in the clinoptilolite is given, where the study of the adsorption efficiency under optimized conditions will be carried out and, subsequently, it will be evaluated in relation to the removal of heavy metals and their antibacterial effects.

2. Experimental Section

The zeolite-type clinoptilolite was collected from Oaxaca, Mexico. It was milled and sieved to −120 + 60 mesh (2 mm).

Subsequently, it was washed with deionized water to remove any impurities and dried at 80 °C for 24 h. Ag nanoparticle solutions were previously prepared according to the chemical reduction method reported widely in the literature [20]. The composite preparation was carried out by immersing 1 g of zeolite into 1 mL of Ag nanoparticles with concentrations of 1, 2, 3 and 4 $mg \cdot L^{-1}$. Each sample was magnetically stirred for different times in intervals of 30 min from 0 to 180 min. The experimental data of the adsorption behavior in zeolite and their chemical characterization was conducted by an atomic absorption spectrophotometry (AAS) technique using Perkin Elmer 3100 equipment. In order to evaluate the adsorption capacity of the zeolite in the optimal conditions, the pH of all aqueous solutions was 8, and it is well known and reported that this pH value favors and generates the maximum adsorption capacity in the zeolite [16–18,21,22]. In the case of chemical characterization, the sample was previously subjected to a digestion and dilution process using lithium metaborate $LiBO_2$. The characterization was complemented by an energy dispersive (EDS) analysis and the AgNP distribution on the zeolite was studied using a Philips Tecnai F20 transmission electron microscope with a field-emission gun attachment. Additionally, a model which proposes the adhesion mechanism of the nanoparticles on the zeolite surface is presented.

3. Results and Discussion

3.1. Chemical Characterization of Natural Zeolite

Figure 1a shows a chemical analysis obtained by EDS, which identified typical elements such as Si, Al, O, Mn, K, and Ca present in the clinoptilolite.

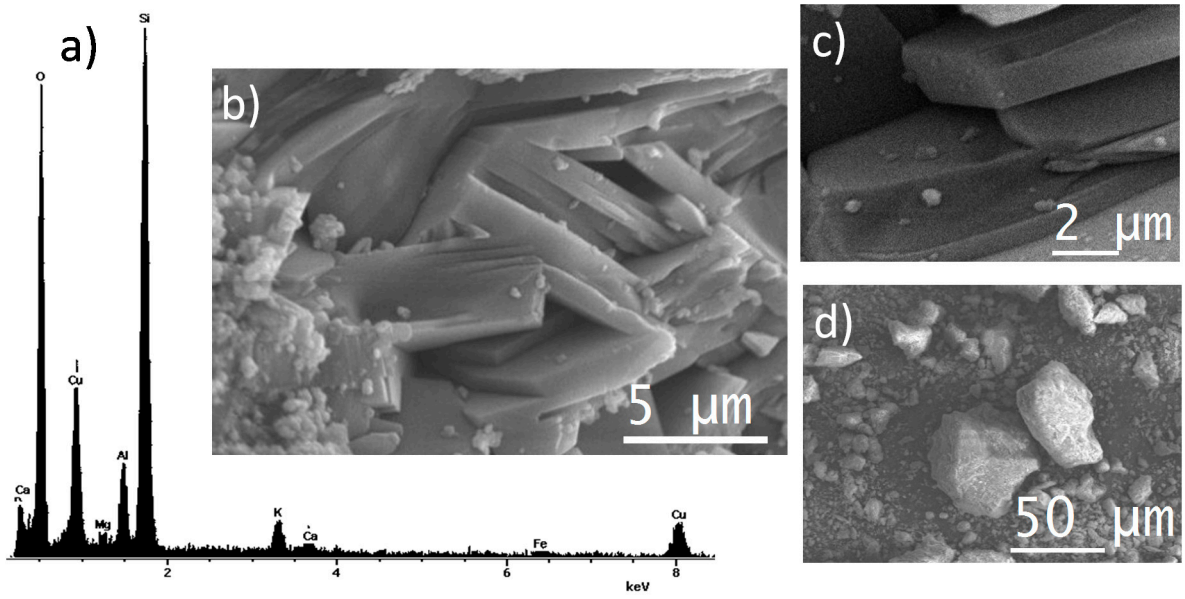

Figure 1. (**a**) EDS chemical analysis of the natural zeolite; (**b**–**d**) Bright-field SEM images corresponding to the clinoptilolite, mordenite, and feldspar phases, respectively.

Figure 1b–d shows bright-field SEM images corresponding to the typical morphologies of the clinoptilolite, mordenite, and feldspar phases reported in previous works [14,23].

In order to perform a precise chemical characterization of the zeolite, Figure 2a–g shows an EDS mapping of the elements present in the zeolite. This analysis is very important because, through this study, we can find the Si/Al ratio of the zeolite. This value can be highly significant to describing the physisorption or chemisorption mechanism presented by the zeolite. However, only with complementary studies of adsorption kinetics is it possible to describe the mechanism of adsorption of silver nanoparticles in zeolite.

As a result of the EDS analysis conducted on the mineral, the elements present in the natural zeolite were identified. However, it is noteworthy that the chemical analysis obtained by the EDS technique is a qualitative analysis. In this sense, a quantitative analysis was performed. To complement it, the quantitative study of the zeolite was performed using the metaborate method as a digestion and dilution mechanism. Subsequently, the absorption spectrophotometry (AAS) technique was used to quantify the elements present in the zeolite. Table 1 shows the quantification of the elements observed in natural zeolite. The relation between Si/Al observed in chemical analysis was 10.19. It has been reported that minerals with a high Si/Al ratio offer an excellent cation exchange capacity [24]. Therefore, it can be affirmed that zeolite exhibits an excellent cation-exchange capacity. However, the adsorption kinetics models presented in this research can describe the specific mechanism of adsorption carried out in the natural zeolite.

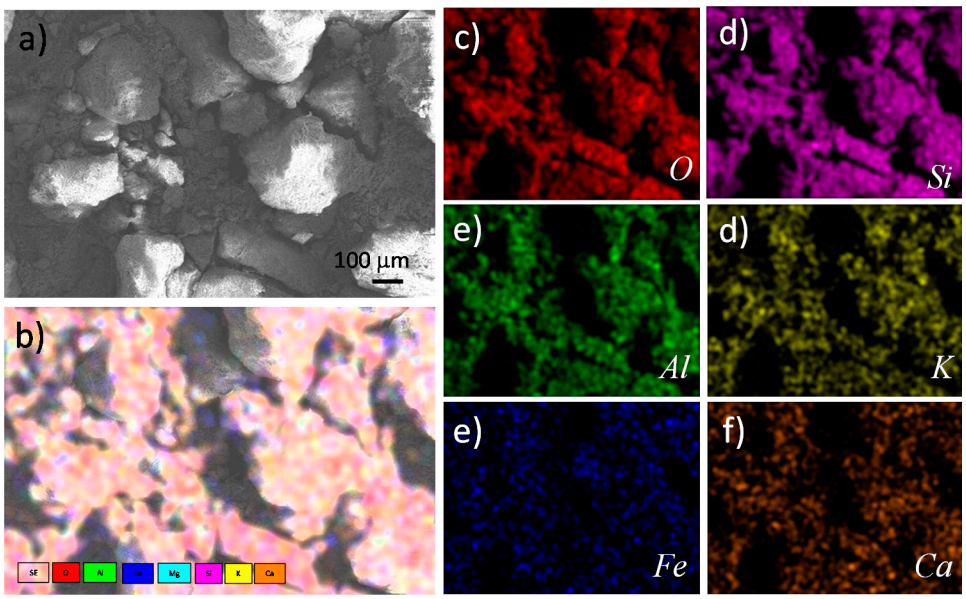

Figure 2. (**a**) SEM micrograph of the zeolite; (**b**) EDS mapping associated with the natural zeolite; and (**c**–**f**) maps of distribution of the elements Si, O, Al, K, Fe, and Ca, respectively.

Table 1. Chemical composition of natural zeolite.

Element	wt. % Zeolite	Oxides	wt. % Zeolite
Si	81.7	SiO_2	77.04
Al	8.01	Al_2O_3	13.2
K	6.04	K_2O	6.42
Fe	1.145	FeO	0.66
Ca	1.2	CaO	0.75
Mg	0.725	MgO	0.53
Na	1.18	Na_2O	1.4

3.2. Experimental Study of the Ag Adsorption by Atomic Absorption Spectrometry (AAS)

3.2.1. Calibration Curves for the Ag Ions and Ag Nanoparticles

To carry out the spectrophotometry analysis, we must first observe a linear behavior in the concentration-absorbance plot according to Beer's law. Calibration curves at concentrations of 1, 2, 3, and 4 $mg \cdot L^{-1}$ were obtained from Ag ions and AgNP solutions, respectively, as shown in Figure 3. Linear behavior in both cases was observed. This behavior is present in a range of 1 to 4 $mg \cdot L^{-1}$, according to the manual operation of the equipment. This result suggests that the solutions of Ag NPs have a linear behavior, similar to that reported for the Ag ionized, and the slopes of the calibration curves for the Ag ions and AgNP solutions were very similar at 0.0265 and 0.0251, respectively. However, the differences between the Ag ions and AgNP solutions were considered and emphasized for subsequent analysis by atomic absorption spectrophotometry. On the other hand, the experimental data obtained from the AgNP solutions, suggest that the flame temperature employed during the ion atomization process was enough for nanoparticle disintegration and, consequently, for forming Ag atomic vapor.

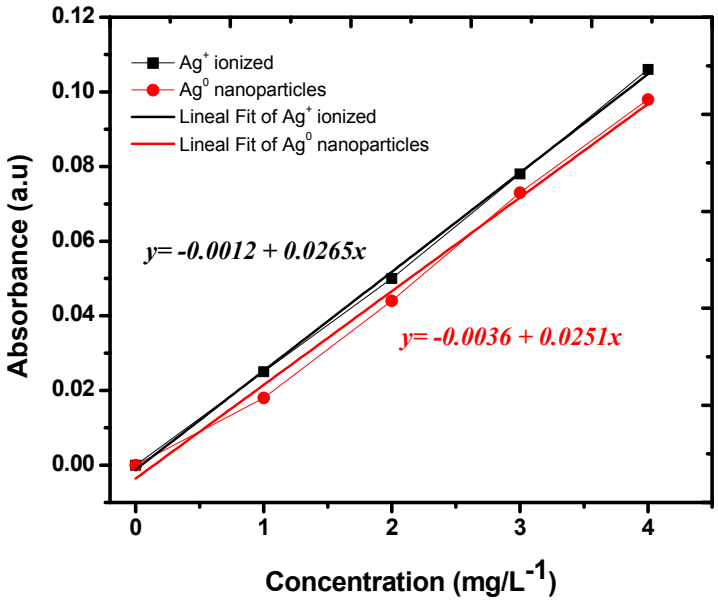

Figure 3. AAS calibration curves associated with the Ag ions and Ag nanoparticles. Experimental data and linear fit.

3.2.2. Adsorption Efficiency of Ag Ions and AgNPs on the Zeolite

Figure 4a shows the AgNP adsorption by clinoptilolite. The highest rates of adsorption are observed in the sample with a concentration of 2 mg·L^{-1}. The value of maximum adsorption is 90% and is conducted over a time of 150 min. For subsequent values of 150 min and 4 mg·L^{-1} no relevant changes are presented in the adsorption rates. This result suggests that zeolite saturation depends directly on the effective diameter of the nanoparticles and, consequently, the volume of AgNPs used for adsorption.

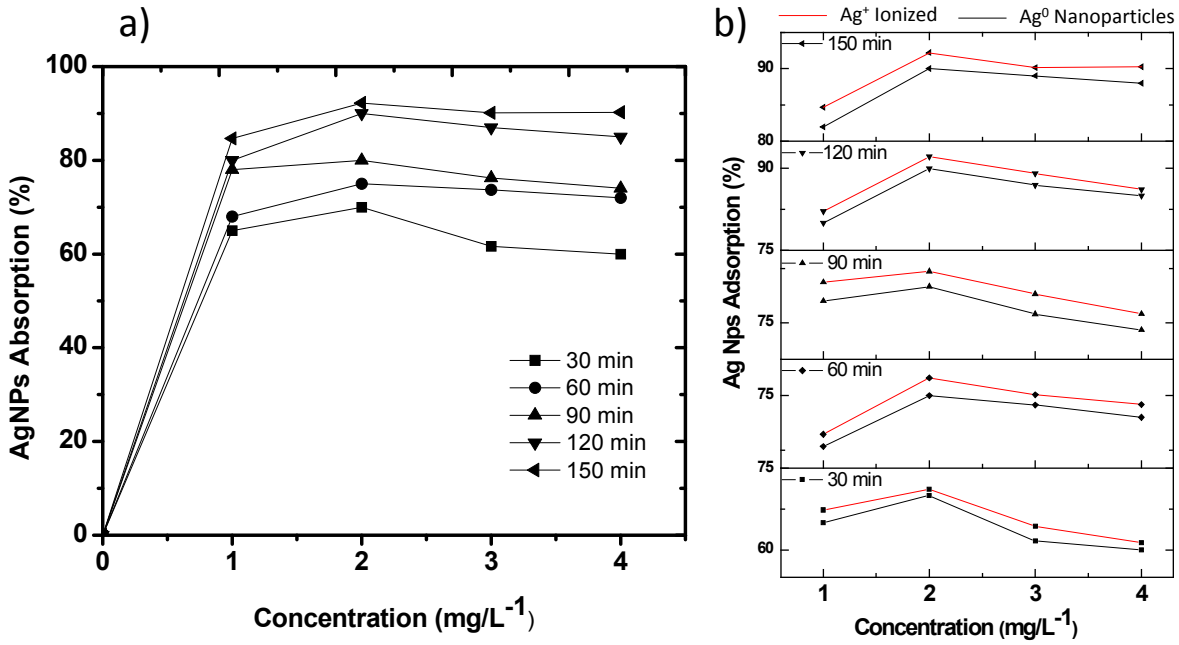

Figure 4. Graphs of the experimental data corresponding to the adsorption efficiency of (**a**) AgNPs and (**b**) AgNPs and Ag ions onto the zeolite.

Some theoretical models are presented below to investigate the mechanism of AgNP sorption onto clinoptilolite. Moreover, the calibration curves obtained for Ag ions and AgNPs show a very similar behavior in both cases (Figure 4b). This can be attributed to the fact that silver nanoparticles with pH values over 6 tend to ionize and, consequently, their adsorption behavior is very similar to that exhibited by the Ag ions [16]. In order to compare the adsorption efficiency of the AgNPs and Ag ions, Figure 4b shows a graph of the adsorption efficiency of these two species. In this case, it can be seen that, for all adsorption times (30–150 min), the Ag ion solutions have a higher adsorption efficiency on the zeolite compared with AgNPs.

3.3. Theoretical Models

The theoretical models reveal the solid/liquid adsorption processes. These processes are generally due to a cation exchange reaction between adsorbent and adsorbate related to a mass-transport process or particle diffusion in macropores or micropores [25]. Pseudo-first-order, pseudo-second-order, Elovich, and intraparticle diffusion models are presented to describe and support the adsorption kinetic behavior of AgNPs.

3.3.1. Lagergren Pseudo-First-Order Model

The pseudo-first-order adsorption model is defined by Lagergren [26,27]

$$\frac{dq}{dt} = K_1(q_e - q_t) \tag{1}$$

where q_e and q_t are the amounts of AgNPs sorbed at equilibrium and a given time t. The pseudo-first-order adsorption rate coefficient is k_1 (min^{-1}). Solving the differential equation for boundary conditions, $t = 0$, $q_t = 0$, $t = t$ and $q_t = q_t$, this equation can be expressed in the linear form as:

$$\ln(q_e - q_t) = lnq_e - kt \tag{2}$$

3.3.2. Pseudo-Second-Order Model

The pseudo-second-order kinetic equation may be expressed as [28,29]

$$\frac{dq}{dt} = K_2(q_e - q_t)^2 \tag{3}$$

Using the integration limits employed in the first-order equation, this equation can be written in the following way:

$$\frac{t}{q_t} = \frac{1}{k_2 {q_e}^2} - \frac{1}{q_e}t \tag{4}$$

In this case, k_2 represents the rate constant for pseudo-second-order sorption ($g \cdot mg^{-1} \cdot min^{-1}$).

3.3.3. Elovich Model

This mathematical model has been widely used in the description of the kinetics of adsorption of a solute in a liquid phase from a solid sorbent. The mathematical expression that governs the behavior of this model is [30]:

$$\frac{dq_t}{dt} = \alpha e^{-\beta q_t} \quad (5)$$

Integrating Equation (3) and using the boundary conditions of the pseudo-first-order model, the Elovich or Roginsky and Zeldovich equation would be:

$$q_t = \frac{1}{\beta}\ln(\alpha\beta) + \frac{1}{\beta} lnt \quad (6)$$

where α is the initial adsorption rate (mg·g^{-1}·min) and β the desorption constant (g·mg^{-1}). In this case, β is described in terms of surface area covered and the activation energy derived from the chemisorption by the adsorbent.

3.3.4. Intraparticle Diffusion Model

The other kinetic equation is the intraparticle diffusion model, given by:

$$q_t = k_i\sqrt{t} + C_i \quad (7)$$

where q_t describes the amount per unit mass of nanoparticles adsorbed by the zeolite at time t, k_i (mg·g^{-1}·min$^{-0.5}$) is the rate constant of intraparticle diffusion, and C_i is the intercept [31,32].

Figure 5a shows the Lagergren kinetics adsorption model of AgNPs into clinoptilolite. In this case, a significant correlation between the experimental results and the R^2 factor is observed (Table 2). The highest correlation values for the first-order Lagergren model are presented in the concentrations of 3 and 4 mg·L^{-1}. This result supports the experimental values shown in Figure 4 where the adsorption efficiency values are similar in both cases and their behavior is linear. Of the employed theoretical models, the pseudo-second-order model (Figure 5b) presents the highest correlation values which are of the order of 0.99. Therefore, the second-order model describes the adsorption process with greater accuracy. This represents chemisorption or chemical adsorption due to the formation of chemical bonds between adsorbent and adsorbate in a monolayer on the surface [26,33].

Table 2. Kinetic parameters obtained from theoretical adsorption models.

Kinetic Model	Lagergren First-Order (K_1) min^{-1}		Pseudo-Second-Order K_2 (g·mg^{-1}·min^{-1}) q_e (mg·g^{-1})		Elovich α (mg·g^{-1}·min) β (g·mg^{-1})		Intraparticle Duffusion K_i (mg·g^{-1}·min$^{-0.5}$)	
1 mg·L^{-1}	K_1	0.023	K_2	1.88×10^{2}	α	73,690.88	C_i	4.93×10^{-4}
			q_e	8.38×10^{-4}	β	0.000115	K_i	2.76×10^{-5}
	R^2	0.762	R^2	0.99108	R^2	0.89589	R^2	0.91193
2 mg·L^{-1}	K_1	0.032	K_2	73.4	α	1.98×10^{4}	C_i	0.00102
			q_e	1.85×10^{-3}	β	2.69×10^{-4}	K_i	6.52×10^{-5}
	R^2	0.857	R^2	0.98635	R^2	0.88164	R^2	0.92399
3 mg·L^{-1}	K_1	0.031	K_2	37.8	α	2.33×10^{3}	C_i	0.0012
			q_e	2.75×10^{-3}	β	5.13×10^{-4}	K_i	1.22×10^{-4}
	R^2	0.907	R^2	0.98026	R^2	0.94803	R^2	0.95313
4 mg·L^{-1}	K_1	0.029	K_2	27.2	α	1.53×10^{3}	C_i	0.00152
			q_e	3.61×10^{-3}	β	6.88×10^{-4}	K_i	1.65×10^{-4}
	R^2	0.908	R^2	0.97719	R^2	0.93829	R^2	0.95237

In this sense, the Elovich model (Figure 5c) also represents a chemisorption phenomenon. Nonetheless, this model is applied to systems with heterogeneous surfaces and different activation energies [9,34]. Consequently, the correlation coefficients obtained by the Elovich model ($0.88164 < R^2 < 0.93829$) exhibit less agreement with the experimental values obtained. The intraparticle diffusion model (Figure 5d) presents R^2 values in the range of $0.911 < R^2 < 0.9523$ (Table 2). This result can be attributed to the homogeneous porous structure of the zeolite. Therefore, this model also describes the transport and diffusion mechanism of the solute through the internal structure of the pores of the adsorbent (clinoptilolite).

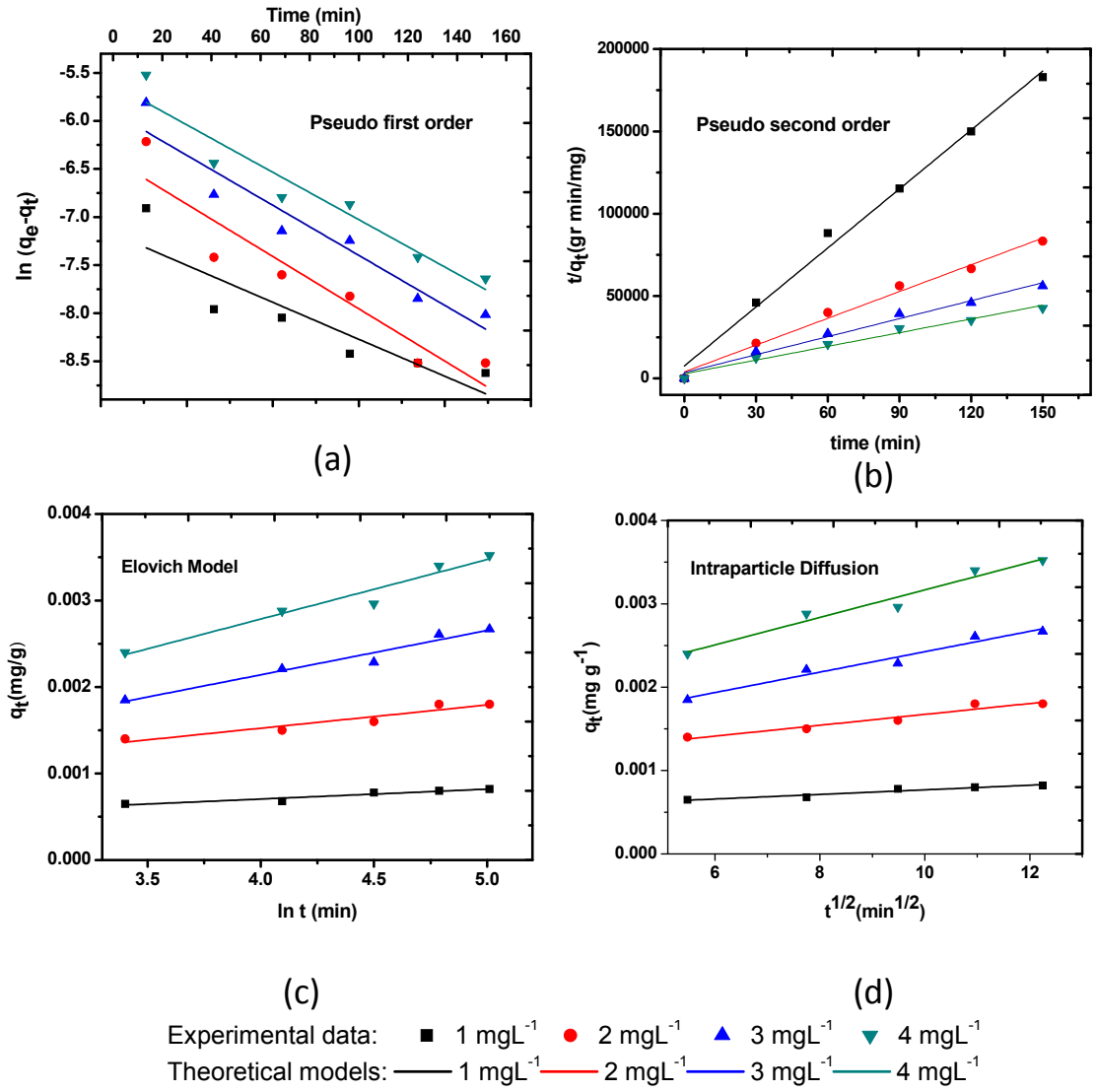

Figure 5. Graphs of the theoretical models corresponding to (**a**) the Lagergren pseudo-first-order model; (**b**) the second-order model; (**c**) the Elovich; and (**d**) the intraparticle diffusion models.

Figure 6 presents the correlation values (R^2) obtained for the theoretical models presented. This graph shows that the highest R^2 values are associated with the pseudo-second-order model. Typically, this model describes a chemisorption process, which involves valence forces generated between the zeolite surface and the active sites of the AgNPs. In this regard, it can be assumed that

the ionization of Ag nanoparticles promotes the superficial adhesion of the AgNPs on the zeolite outer surface.

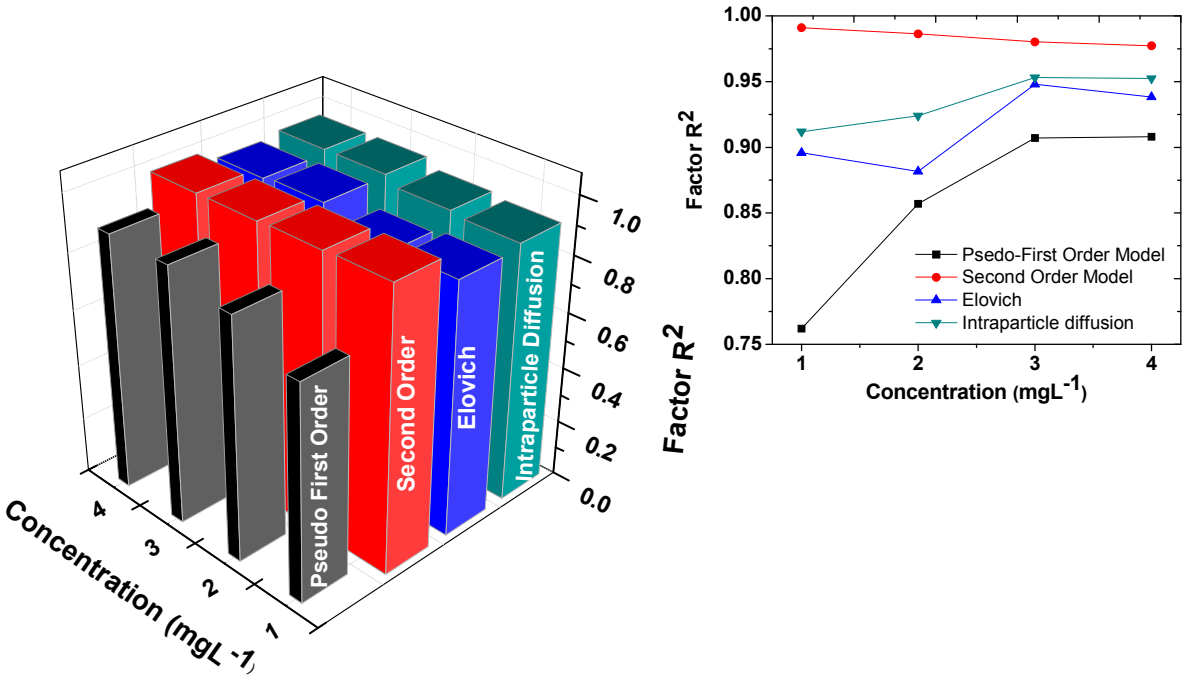

Figure 6. Analysis of the R^2 correlation values obtained from the theoretical models employed to describe the AgNPs adsorption process on zeolite.

In order to study the distribution of silver nanoparticles on the surface of the zeolite, a study by TEM was performed. Figure 7 shows a (a) bright-field TEM and (b) STEM images, in which the distribution of the AgNPs on the zeolite outer surface can be appreciated. This result verifies that the chemisorption phenomenon describes the adsorption process carried out by the mineral. This is due to the AgNPs' interaction with the active sites of the zeolite, and the formation of a uni-molecular layer uniformly distributed on the zeolite outer surface is observed. In this sense, it can be deduced that the process of impregnation of the particles was carried out efficiently since the adsorbate was distributed throughout the external surface of the zeolite.

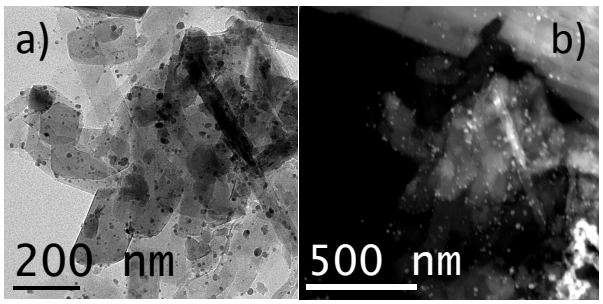

Figure 7. (**a**) Bright-field TEM and (**b**) STEM images corresponding to the AgNP distribution onto the zeolite surface.

For additional evidence of the chemisorption process, Figure 8 schematizes the adhesion mechanism of the AgNPs on the clinoptilolite surface, which was carried out by the interaction of the

valence forces as describe in the pseudo-second-order model. Also, this proposed model is in accordance with the results observed by the TEM images. The model was performed using the software QUANTA (Accelrys, San Diego, CA, USA).

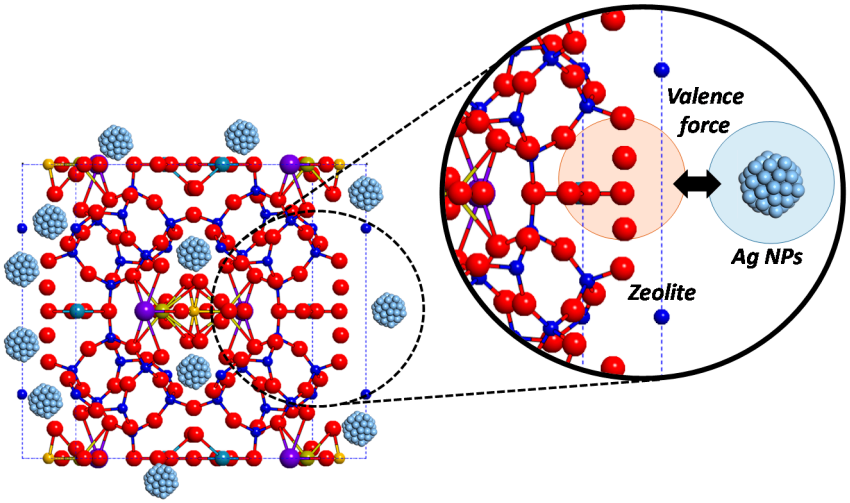

Figure 8. Ball-and-stick model proposed for the adhesion mechanism of the AgNPs on the clinoptilolite surface.

4. Conclusions

The interaction between the zeolite and the AgNPs is described through a chemisorption process. In this research, the characteristics of this process are observed and verified by adsorption theoretical models. Pseudo-second-order and intraparticle diffusion models present higher correlation factors with respect to the experimental values obtained. This fact supports the formation of chemical bonds between the adsorbent and the adsorbate in a monolayer on the zeolite surface. The homogeneous mineral porosity promotes this behavior. On the other hand, the high adsorption efficiencies observed verified the affinity of the zeolite and the AgNPs. Minor particle concentrations (1 and 2 $mg \cdot L^{-1}$) present high adsorption rates, due to the fact that the pore saturation is lower, promoting the adsorption phenomenon.

Author Contributions

Alvaro de Jesús Ruíz and Ramiro Pérez conceived and designed the experiments, Alvaro Ruíz performed experiments, Alvaro de Jesus Ruíz and Ramiro Pérez analysed the data. Alvaro de Jesús Ruíz wrote the paper and Ramiro Pérez revised the manuscript.

Conflicts of Interest

The authors declare no conflict of interest.

References

1. Khajeh-Talkhoncheh, S.; Haghighi, M. Syngas production via dry reforming of methane over Ni-based nanocatalyst over various supports of clinoptilolite, ceria and alumina. *J. Nat. Gas Sci. Eng.* **2015**, *23*, 16–25.
2. Romero, D.; Chlala, D.; Labaki, M.; Royer, S.; Bellat, J.-P.; Bezverkhyy, I.; Giraudon, J.-M.; Lamonier, J.-F. Removal of Toluene over NaX Zeolite Exchanged with Cu^{2+}. *Catalysts* **2015**, *5*, 1479–1497.
3. Munthali, M.; Elsheikh, M.; Johan, E.; Matsue, N. Proton Adsorption Selectivity of Zeolites in Aqueous Media: Effect of Si/Al Ratio of Zeolites. *Molecules* **2014**, *19*, 20468–20481.
4. Ajoudanian, N.; Nezamzadeh-Ejhieh, A. Enhanced photocatalytic activity of nickel oxide supported on clinoptilolite nanoparticles for the photodegradation of aqueous cephalexin. *Mater. Sci. Semicond. Process.* **2015**, *36*, 162–169.
5. Donati, E.; Polcaro, C.M.; Ciccioli, P.; Galli, E. The comparative study of a laccase-natural clinoptilolite-based catalyst activity and free laccase activity on model compounds. *J. Hazard. Mater.* **2015**, *289*, 83–90.
6. Rodríguez-Iznaga, I.; Petranovskii, V.; Castillón-Barraza, F.; Concepción-Rosabal, B. Copper-Silver Bimetallic System on Natural Clinoptilolite: Thermal Reduction of Cu^{2+} and Ag^{+} Exchanged. *J. Nanosci. Nanotechnol.* **2011**, *11*, 5580–5586.
7. Fateminia, F.S.; Falamaki, C. Zero valent nano-sized iron/clinoptilolite modified with zero valent copper for reductive nitrate removal. *Process Saf. Environ. Prot.* **2013**, *91*, 304–310.
8. Karel, F.B.; Koparal, A.S.; Kaynak, E. Development of Silver Ion Doped Antibacterial Clays and Investigation of Their Antibacterial Activity. *Adv. Mater. Sci. Eng.* **2015**, *2015*, 1–6.
9. Guaya, D.; Valderrama, C.; Farran, A.; Armijos, C.; Cortina, J.L. Simultaneous phosphate and ammonium removal from aqueous solution by a hydrated aluminum oxide modified natural zeolite. *Chem. Eng. J.* **2015**, *271*, 204–213.
10. Pourtaheri, A.; Nezamzadeh-Ejhieh, A. Enhancement in photocatalytic activity of NiO by supporting onto an Iranian clinoptilolite nano-particles of aqueous solution of cefuroxime pharmaceutical capsule. *Spectrochim. Acta A Mol. Biomol. Spectrosc.* **2015**, *137*, 338–344.
11. Zayed, M.A.; El-Begawy, S.E.M.; Hassan, H.E.S. Enhancement of stabilizing properties of double-base propellants using nano-scale inorganic compounds. *J. Hazard. Mater.* **2012**, *227–228*, 274–279.
12. Nezamzadeh-Ejhieh, A.; Shirvani, K. CdS Loaded an Iranian Clinoptilolite as a Heterogeneous Catalyst in Photodegradation of *p*-Aminophenol. *J. Chem.* **2013**, *2013*, 1–11.
13. Ortiz-Polo, A.; Richards-Uribe, R.M.; Otazo-Sánchez, E.M.; Prieto-García, F.; Hernández-Ávila, J.; Acevedo-Sandoval, O.; Gordillo-Martínez, A. New organo-inorganic materials for water contaminants remediation. In Proceedings of the Materials Research Society Symposium Proceedings, San Francisco, CA, USA, 9 April 2008; Volume 1007, pp. 129–136.
14. Jiménez-Cedillo, M.J.; Olguín, M.T.; Fall, C.; Colín, A. Adsorption capacity of iron- or iron-manganese-modified zeolite-rich tuffs for As(III) and As(V) water pollutants. *Appl. Clay Sci.* **2011**, *54*, 206–216.

15. Top, A.; Ülkü, S. Silver, zinc, and copper exchange in a Na-clinoptilolite and resulting effect on antibacterial activity. *Appl. Clay Sci.* **2004**, *27*, 13–19.
16. Çoruh, S.; Şenel, G.; Ergun, O.N. A comparison of the properties of natural clinoptilolites and their ion-exchange capacities for silver removal. *J. Hazard. Mater.* **2010**, *180*, 486–492.
17. Lihareva, N.; Dimova, L.; Petrov, O.; Tzvetanova, Y. Ag^+ sorption on natural and Na-exchanged clinoptilolite from Eastern Rhodopes, Bulgaria. *Microporous Mesoporous Mater.* **2010**, *130*, 32–37.
18. Praus, P.; Turicová, M.; Machovič, V.; Študentová, S.; Klementová, M. Characterization of silver nanoparticles deposited on montmorillonite. *Appl. Clay Sci.* **2010**, *49*, 341–345.
19. Fechete, I.; Vedrine, J. Nanoporous Materials as New Engineered Catalysts for the Synthesis of Green Fuels. *Molecules* **2015**, *20*, 5638–5666.
20. Pal, B.; Rana, S.; Kaur, R. Influence of Different Reducing Agents on the Ag Nanostructures and Their Electrokinetic and Catalytic Properties. *J. Nanosci. Nanotechnol.* **2015**, *15*, 2753–2760.
21. Chiericatti, C.; Basílico, J.C.; Basílico, M.L.Z.; Zamaro, J.M. Antifungal activity of silver ions exchanged in mordenite. *Microporous Mesoporous Mater.* **2014**, *188*, 118–125.
22. Taylor, P.; Lihareva, N.; Tzvetanova, Y.; Petrov, O.; Dimova, L. Sorption of Silver Cations by Natural and Na-Exchanged Mordenite Sorption of Silver Cations by Natural and Na-Exchanged Mordenite. *Sep. Sci. Technol.* **2015**, *6395*, 37–41.
23. De la Rosa-Gómez, I.; Olguín, M.T.; Alcántara, D. Bactericides of coliform microorganisms from wastewater using silver-clinoptilolite rich tuffs. *Appl. Clay Sci.* **2008**, *40*, 45–53.
24. Celik, F.E.; Kim, T.-J.; Bell, A.T. Effect of zeolite framework type and Si/Al ratio on dimethoxymethane carbonylation. *J. Catal.* **2010**, *270*, 185–195.
25. Mihaly-Cozmuta, L.; Mihaly-Cozmuta, A.; Peter, A.; Nicula, C.; Tutu, H.; Silipas, D. Adsorption of heavy metal cations by Na-clinoptilolite: Equilibrium and selectivity studies. *J. Environ. Manag.* **2014**, *137*, 69–80.
26. Sen, S.; Bhattacharyya, K.G. Kinetics of adsorption of metal ions on inorganic materials: A review. *Adv. Colloid Interface Sci.* **2011**, *162*, 39–58.
27. Goldani, E.; Moro, C.C.; Maia, S.M. A Study Employing Differents Clays for Fe and Mn Removal in the Treatment of Acid Mine Drainage. *Water Air Soil Poll.* **2013**, *224*, 1–11.
28. Ho, Y.S.; Mckay, G. Pseudo-second order model for sorption processes. *Process Biochem.* **1999**, *34*, 451–465.
29. Zhang, S.; Wang, D.; Chen, Y.C.; Zhang, X.W.; Chen, G.J. Adsorption of calcium ion from aqueous solution using Na^+-conditioned clinoptilolite for hot-water softening. *Huanjing Kexue* **2015**, *36*, 744–750.
30. Cortés-Martínez, R.; Olguín, M.T.; Solache-Ríos, M. Cesium sorption by clinoptilolite-rich tuffs in batch and fixed-bed systems. *Desalination* **2010**, *258*, 164–170.
31. Olad, A.; Ahmadi, S.; Rashidzadeh, A. Removal of Nickel(II) from aqueous solutions with polypyrrole modified clinoptilolite: Kinetic and isotherm studies. *Desalin. Water Treat.* **2013**, *51*, 7172–7180.
32. O'Carroll, D.; Sleep, B.; Krol, M.; Boparai, H.; Kocur, C. Nanoscale zero valent iron and bimetallic particles for contaminated site remediation. *Adv. Water Resour.* **2013**, *51*, 104–122.

33. Anari-Anaraki, M.; Nezamzadeh-Ejhieh, A. Modification of an Iranian clinoptilolite nanoparticles by hexadecyltrimethyl ammonium cationic surfactant and dithizone for removal of Pb(II) from aqueous solution. *J. Colloid Interface Sci.* **2015**, *440*, 272–281.
34. Yu, Y.; Shapter, J.G.; Popelka-Filcoff, R.; Bennett, J.W.; Ellis, A.V. Copper removal using bio-inspired polydopamine coated natural zeolites. *J. Hazard. Mater.* **2014**, *273*, 174–182.